



Generalized Fundamental Diagram with Implications of Congestion Mitigation

Qianwen Li¹ and Xiaopeng Li, Ph.D., M.ASCE²

Abstract: The classic triangular fundamental diagram describes the functional relationship between flow rate and traffic density for longitudinal movements of homogeneous traffic. This study generalized the classic triangular fundamental diagram in the congestion regime to consider lateral lane-changing and heterogeneous traffic. *F*-test results indicated that the generalized model fit and predicted flow rate better than the classic model. The inconsistency in the literature regarding the impacts of lane changing was reconciled as follows. Lane changes decreased flow rate when traffic was both slightly and severely congested but increased flow rate when traffic was moderately congested. Motivated by this finding, a dynamic lane-changing management strategy was developed to mitigate congestion. Results showed that the proposed strategy improved throughput by 10.3%, average speed by 9.7%, and average delay by 19.2%. The findings from this study advance knowledge of the classic two-dimensional fundamental diagram, reveal the nonlinear effects of lane changes, and provide policy implications for congestion mitigation. **DOI:** 10.1061/JTEPBS.0000658. © 2022 American Society of Civil Engineers.

Author keywords: Fundamental diagram; Lane changing; Heterogeneous traffic; Generalized linear regression; Interaction term.

Introduction

© ASCE

The classic triangular fundamental diagram is the foundation of traffic flow theory in transportation research (Eliasson 2021; Zheng 2021). It describes the relationship between traffic flow (or traffic volume) and traffic density for longitudinal movements of traffic comprising homogeneous vehicles (Newell 1993; Treiber and Kesting 2013). It has been widely used to describe traffic dynamics and to develop congestion control strategies (Qu et al. 2017; Zhang et al. 2018). Despite its popularity, the classic triangular fundamental diagram may not always perfectly describe or predict real-world traffic dynamics due to certain limitations, including the following two major issues.

First, the classic triangular fundamental diagram only focuses on vehicle longitudinal interactions (i.e., car-following dynamics) without adequately addressing impacts from latitudinal interactions (i.e., lane-changing behavior). However, it has been shown that lane-changing behavior may significantly impact traffic flow and that the impacts are inconsistent among existing studies (Aghabayk et al. 2011; Li et al. 2021). On the one hand, several studies have stated that lane-changing behavior deteriorates traffic flow by generating shock waves on upstream traffic (Zheng 2014; Zheng et al. 2013), causing capacity drops (Coifman et al. 2005; Laval and Daganzo 2006; Zhang et al. 2019), and inducing traffic accidents (Ali et al. 2019; Gu et al. 2019; van Winsum et al. 1999). On the other hand, some studies have found that lane-changing behavior increases flow rate. It has been found that a considerable number of lane changes are triggered by the heterogeneity between lanes (Jin 2010a; Laval and Chilukuri 2016). Lane changes can have balancing effects by smoothing out differences between lanes. Such balancing effects can be beneficial to the overall traffic system in achieving better traffic efficiency, meaning greater flow rate (Cheu et al. 2009; Li et al. 2006; Patire and Cassidy 2011; Shvetsov and Helbing 1999). Overall, the inconsistent impacts of lane changing on traffic flow need to be reconciled.

The studies mentioned qualitatively addressed either positive or negative impacts of lane-changing behavior on traffic flow rate. Only a few attempts have been made to quantitively assess those impacts. Jin (2010a) proposed a lane-changing intensity variable. They assumed that a lane-changing vehicle's contribution to traffic density was doubled and incorporated an intensity-density relationship into the triangular fundamental diagram to capture the negative impacts of lane changes. Jin (2010b) developed a new interpretation of lane-changing intensity following Edie's definition of traffic density. Traffic flow reduction rates caused by lane changes in different time intervals, cell sizes, and locations were calculated, respectively. Jin (2013) proposed a multicommodity Lighthill-Whitham-Richards model for lane-changing traffic and derived a corresponding fundamental diagram with lane changes reducing traffic flow. While these studies provided reasonable explanations as powerful tools to measure the negative impacts of lane changing, possible positive impacts were not captured. The studies just described lay solid foundations for analyzing traffic flow, but the inconsistency between the positive and negative impacts of lane changing on traffic flow from different studies was not reconciled.

Second, the classic triangular fundamental diagram deals with homogeneous traffic of the same vehicle type (Laval and Chilukuri 2016; Qian et al. 2017) so that it is not directly applicable to heterogeneous traffic with various vehicle types, such as passenger cars, trucks, and motorcycles. The passenger car equivalent (PCE) factor has been used in the *Highway Capacity Manual* to convert heterogeneous traffic into homogeneous traffic (Pompigna and Rupi 2015). However, the effects of different vehicle types on traffic flow vary with traffic situation and vehicle length, which cannot be well addressed by the PCE factor (Khan and Maini 1999; Zhou et al. 2019). To address this issue, a variety of models have been proposed to investigate heterogeneous traffic properties. These include continuum models (Gupta and Katiyar 2007; Zhang and Jin 2002),

¹Ph.D. Candidate, Dept. of Civil and Environmental Engineering, Univ. of South Florida, Tampa, FL 33620. Email: qianwenli@usf.edu

²Associate Professor, Dept. of Civil and Environmental Engineering, Univ. of South Florida, Tampa, FL 33620 (corresponding author). ORCID: https://orcid.org/0000-0002-5264-3775. Email: xiaopengli@usf.edu

Note. This manuscript was submitted on October 10, 2021; approved on December 9, 2021; published online on March 11, 2022. Discussion period open until August 11, 2022; separate discussions must be submitted for individual papers. This paper is part of the *Journal of Transportation Engineering*, *Part A: Systems*, © ASCE, ISSN 2473-2907.

car-following models (Mason and Woods 1997; Peeta et al. 2005), and cellular automata models (Qian et al. 2017; Yang et al. 2015). Zhang and Jin (2002) used kinematic wave theory to propose an extended speed-density relation for the triangular fundamental diagram while considering passenger cars and trucks. Yang et al. (2015) adopted the cellular automaton to model the triangular fundamental diagram for different car-truck following combinations. Logghe and Immers (2008) developed a multiclass model where vehicle classes interacted in noncooperative equilibrium. The interaction of classes was considered an assignment of road space to these classes. Qian et al. (2017) generalized the classic cell transmission model to develop a macroscopic heterogeneous flowdensity model. Road capacity split and perceived equivalent density were proposed to model interactions among different vehicle types. While these studies enabled flexible applications of the triangular fundamental diagram to heterogeneous traffic, lane changing was not explicitly incorporated. It is still unclear how lane changing and traffic heterogeneity jointly impact traffic flow.

To bridge the research gaps, this study generalized the classic triangular fundamental diagram (the classic model for short) in the congestion regime to consider lateral lane-changing behavior and heterogeneous traffic. The generalized fundamental diagram was obtained by applying a generalized linear regression model with interaction terms to the next-generation simulation (NGSIM) US101 data set (Federal Highway Administration 2005b).

F-test results showed that the generalized model fit and predicted flow rate better than the classic model. With the interaction terms, the nonlinear effect of lane-changing behavior on flow rate was formulated into a quadratic function of traffic density. The regression results revealed that lane changes decrease flow rate when traffic is slightly and severely congested but increase flow rate when traffic is moderately congested. This finding unifies both positive and negative impacts of lane changing on traffic flow in the same model structure. Further, the spatial transferability of the generalized model was verified with the NGSIM I-80 trajectory data set (Federal Highway Administration 2005a) through a likelihood ratio test.

Motivated by different impacts of lane changing on traffic flow, a dynamic lane-changing management strategy was developed to improve highway mobility, and the performance of the strategy was tested by simulations. The findings advance knowledge of the classic two-dimensional fundamental diagram, reveal the nonlinear effects of lane changes, and shed light on ways to mitigate traffic congestion.

The rest of this paper is organized as follows. The generalized linear regression model with interaction terms is presented and then the model performance measurements are modeled. Next, the NGSIM trajectory data set is introduced, the data aggregation process is described, and the variable statistics are presented. The generalized fundamental diagram model results are next presented, followed by an assessment of the generalized model's spatial transferability using the NGSIM I-80 trajectory data set. Following are tests of the performance of the dynamic lane-changing management strategy with simulations and finally conclusions and future research directions.

Methodology

The methodology is outlined in Fig. 1. The classic model was formulated with flow rate and density. The generalized model was formulated to include lane changes and vehicle types. The NGSIM US101 data set was used to estimate these models and the estimation results were evaluated. Model prediction accuracy was also

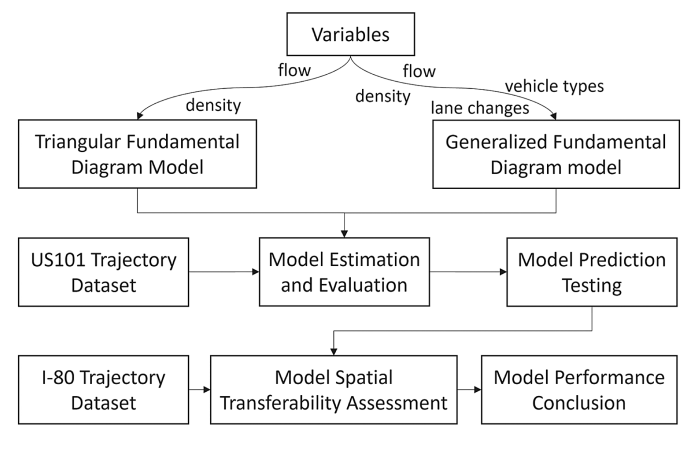


Fig. 1. Methodology logic.

tested. Next, the NGSIM I-80 data set was used to assess spatial transferability. Finally, it was concluded that the generalized fundamental diagram model better fits and predicts flow rate and is spatially transferable.

Linear regression was adopted to model traffic flow rate in this study. Because of its simplicity and superior interpretability, it is an extensively used statistical approach to model the relationship between one continuous response and one or more explanatory variables. The typical linear regression model is formulated as (Washington et al. 2020)

$$Y_{n\times 1} = X_{n\times p} \beta_{p\times 1} + \varepsilon_{n\times 1} \tag{1}$$

where Y, X, and β = response matrix, explanatory matrix, and parameter matrix respectively; ε = disturbance term; n = number of observations; and p = number of variables included in the model.

The typical linear regression model assumes that all explanatory variables are independent of each other. This assumption does not hold when the effect of one explanatory variable on the response depends on the value of another explanatory variable. For example, the effect of lane changing on flow rate is associated with density. In this case, the typical linear regression model is not applicable but needs to be generalized by adding interaction terms (Cortina 1993; Karaca-Mandic et al. 2012) between the correlated variables. The interaction term is constructed by computing the product of the interacting explanatory variables—for example, $x_i \times x_j$, where $i \neq j$. The generalized linear regression model with interaction terms can be formulated as

$$Y_{n\times 1} = X_{n\times p} \beta_{p\times 1} + Z_{n\times q} \beta_{q\times 1}' + \varepsilon_{n\times 1}$$
 (2)

where Y, X, β , Z, and β' = response matrix, explanatory matrix, explanatory parameter matrix, interaction matrix, and interaction parameter matrix, respectively; ε = disturbance term; n = number of observations; p =number of explanatory variables included in the model; and q = number of interaction terms included in the model.

The marginal effect is used to determine the effect of a one-unit change in an explanatory variable on the response. It is obtained by calculating the partial derivative of the response with respect to the explanatory variable while other explanatory variables are held constant.

The adjusted R^2 is used to evaluate model fitness and is formulated as

J. Transp. Eng., Part A: Systems

Adjusted
$$R^2 = 1 - \frac{(1 - R^2)(N - 1)}{N - p - 1}$$
 (3)

where

$$R^{2} = 1 - \frac{\sum_{i=1}^{N} (y_{i} - y_{i}')^{2}}{\sum_{i=1}^{N} (y_{i} - \bar{y})^{2}}$$
(4)

where y_i = observed value; \bar{y} = mean of all observed values; y'_i = predicted value; and N = number of observations. The root-mean square error (RMSE) is used to measure model prediction accuracy. It is calculated as

$$RMSE = \sqrt{\frac{\sum_{i=1}^{N} (y_i' - y_i)^2}{N}}$$
 (5)

where y_i = observed value; y_i' = predicted value; and N = number of observations.

Empirical Settings

This section briefly introduces the NGSIM US101 trajectory data set, describes the data aggregation process, and presents descriptive statistics of the observation set.

NGSIM Trajectory Data Set

The NGSIM US101 trajectory data set used in this study was collected on the Hollywood Freeway, in Los Angeles, California, on June 15, 2005 (https://www.fhwa.dot.gov/publications/research /operations/07030/07030.pdf). The study area is about 640 m long consisting of 5 main lanes (Lanes 1–5), one auxiliary lane (Lane 6), one on-ramp (Lane 7), and one off-ramp (Lane 8). Eight synchronized digital video cameras were mounted on a building adjacent to the freeway to record vehicles passing through the segment. Vehicles' trajectories were extracted from the video every 1/10 s. The data set contains 45-min of trajectory data, divided into three periods: 7:50 to 8:05 a.m.; 8:05 to 8:20 a.m.; and 8:20 to 8:35 a.m. The current study focused on vehicle trajectories in the five main lanes to capture lane changes from the segment start to the segment end. Following previous literature, this study did not further classify lane changes into mandatory and discretionary (Cheu et al. 2009; Jin 2010a, 2013; Li et al. 2006).

Data Aggregation

When vehicle trajectory data are available, Edie's equations can be used to calculate macroscopic traffic variables with a subset of trajectories in an arbitrary time-space region (Knoop et al. 2012; Laval 2011). Then traffic flow rate q, traffic density k, and average space-mean speed v are formulated as follows, respectively:

$$q = \sum_{i=1}^{I} \frac{x_i}{|A|} \tag{6}$$

$$k = \sum_{i=1}^{I} \frac{t_i}{|A|} \tag{7}$$

$$v = \frac{q}{k} = \frac{\sum_{i=1}^{I} \frac{x_i}{|A|}}{\sum_{i=1}^{I} \frac{t_i}{|A|}}$$
 (8)

where A = arbitrary region containing I vehicles, indexed from 1 to I; |A| = area of region A; $x_i =$ distance vehicle i travels in region A; and $t_i =$ time vehicle i spends in region A.

We divided the time-space diagram into parallelograms with a base of 20 s and a height of 60 m. Each parallelogram denoted a region A—that is, an observation—as illustrated in Fig. 2. Two opposite sides of the parallelogram had slopes of the shockwave speed (18 km/h in this data set) and the other two sides were horizontal with zero slopes. The parallelogram needed to be large enough to accommodate lane changes. The dimensions were chosen because they produced the most significant statistical results. Only parallelograms filled with trajectories were included in the observation set.

Observation Set

In total, 837 observations (837 regions) were obtained from the above data aggregation. The variables in Table 1 were extracted correspondingly. Traffic flow rate and space-mean speed were defined in the previous subsection. Truck percentage was calculated as number of trucks/total number of vehicles in region $A \times 100\%$. Motorcycle percentage was calculated as number of motorcycles/total number of vehicles in region $A \times 100\%$. Lane-changing rate was calculated as number of lane changes (N^{LC}) /total number of vehicles (N^{veh}) in region $A \times 100\%$. Two consecutive lane changes by the same vehicle were not counted when the vehicle switched

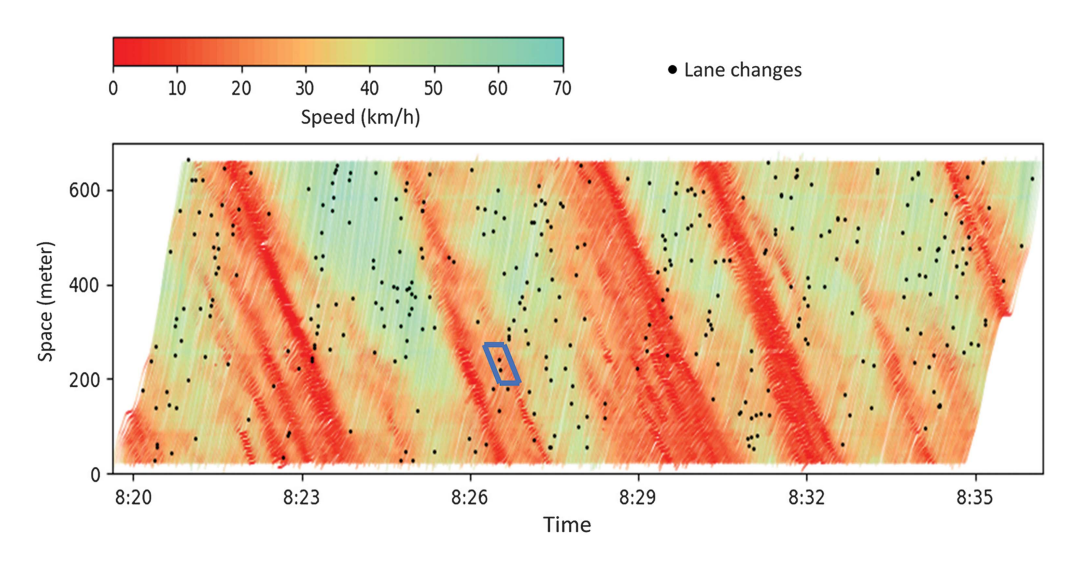


Fig. 2. Observation.

Table 1. Descriptive statistics of variables

Variable	Minimum	Maximum	Mean	Standard deviation
Dependent variable				_
Traffic flow rate (veh/h/ln)	731	1,794	1,419	218
Independent variable				
Density (veh/km/ln)	21	80	44	12
Truck percentage	0	6.08	2.02	1.26
Motorcycle percentage	0	6.76	0.76	1.35
Lane-changing rate $\left(100\% \times \frac{N^{LC}}{N^{veh}}\right)$	0	5.44	0.86	0.96

Source: Data from Federal Highway Administration (2005b).

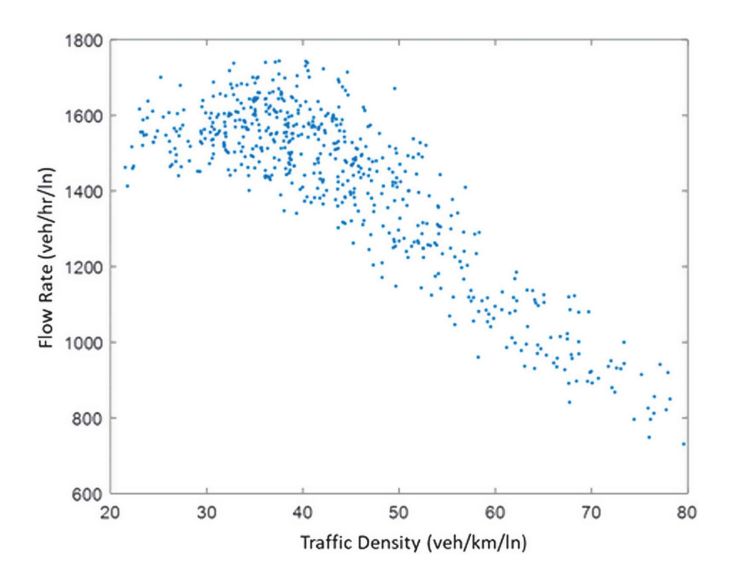


Fig. 3. Flow and density relationship. (Data from Federal Highway Administration 2005b.)

back to its original lane shortly after its first lane change. These were false lane changes probably due to identification errors (Jin 2010b). Vehicle trajectories were plotted to exclude false lane changes. Descriptive statistics of these variables are provided in Table 1. The relationship of flow and density is plotted in Fig. 3.

Generalized Fundamental Diagram Model

This section first compares the performance of several generalized fundamental diagram models with that of the classic model and then presents detailed results.

Seventy percent of the observations (586 regions) were used to estimate four fundamental diagram models. The model fitness results (i.e., the adjusted R^2 values) are provided in Table 2. The four estimated models were employed on the remaining 30% of the

observations (251 regions) to compare flow rate prediction accuracy (RMSE of flow rate in Table 2). We highlight two points here.

First, lane-changing rates in Models 3 and 4 were endogenous variables affected by traffic density. In this case, ordinary least squares could produce biased estimation results. One way to avoid this is to identify instrumental variables; however, this approach was difficult to apply to the investigated problem. As an alternative, we opted to use interaction terms since it has been proven that the functional form of an interaction model naturally leads to alternative instrumental variables (Bun and Harrison 2019).

Second, despite the inclusion of the first interaction term $lcr \times k$, the second interaction term $lcr \times k^2$ was introduced in Models 3 and 4 to reconcile the inconsistency between the positive and negative impacts of lane changing on traffic flow from different studies. The statistically significant t statistics justified this inclusion. Higher-order interaction terms were tested but were not statistically significant.

It was shown that Models 2, 3, and 4 fitted and predicted flow rate better than Model 1 (the classic fundamental diagram), indicated by the higher adjusted R^2 and the lower RMSE values. Accounting for heterogeneous traffic slightly improved flow rate fitness and prediction accuracy, as shown by the results of Model 2. Considering lane-changing behavior greatly improved flow rate fitness and prediction accuracy, as shown by the results of Model 3. The best model performance was observed after incorporating both lane-changing behavior and heterogeneous traffic, as shown by the results of Model 4. One could argue that including more predictors leads to better model performance. Thus, we conducted three hypothesis tests to test the superiority of Model 4. Three null hypotheses (H_{01} , H_{02} , and H_{03}) and three corresponding alternative hypotheses (H_{a1} , H_{a2} , and H_{a3}) were proposed.

• Hypothesis test to compare Model 4 and Model 1:

 H_{01} : Model 4 does not fit flow rate statistically better than Model 1.

H_{a1}: Model 4 fits flow rate statistically better than Model 1.

• Hypothesis test to compare Model 4 and Model 2:

 ${
m H}_{02}$: Model 4 does not fit flow rate statistically better than Model 2.

Table 2. Fundamental diagram model comparison

Model index	Model formulation	Adjusted R ²	RMSE (veh/h/ln)
1	$q = c + \alpha_1 \times k$	0.730	114.453
2	$q = c + \beta_1 \times k + \beta_2 \times p_{\text{truck}} + \beta_3 \times p_{\text{cycle}}$	0.735	112.004
3	$q = c + \gamma_1 \times k + \gamma_2 \times lcr + \gamma_3 \times lcr \times k + \gamma_4 \times k^2 \times lcr$	0.768	106.780
4	$q = c + \mu_1 \times k + \mu_2 \times lcr + \mu_3 \times lcr \times k + \mu_4 \times k^2 \times lcr + \mu_5 \times p_{\text{truck}} + \mu_6 \times p_{\text{cycle}}$	0.771	104.153

Source: Data from Federal Highway Administration (2005b).

Note: q = flow rate; k = traffic density; lcr = lane-changing rate; $p_{\text{truck}} =$ truck percentage; $p_{\text{cycle}} =$ motorcycle percentage; c = constant; α , β , γ , $\mu =$ model parameters; and $lcr \times k$, $lcr \times k^2 =$ interaction terms.

H_{a2}: Model 4 fits flow rate statistically better than Model 2.
 Hypothesis test to compare Model 4 and Model 3:

 ${
m H}_{03}$: Model 4 does not fit flow rate statistically better than Model 3.

 H_{a3} : Model 4 fits flow rate statistically better than Model 3. Since Model 4 (the full model) has more than one additional term than do Models 1, 2, and 3 (the restricted models), the F-test was adopted (Ludden et al. 1994)

$$F = \frac{SSE_{\text{restricted}} - SSE_{\text{full}}}{SSE_{\text{full}}} \times \frac{N - P_{\text{full}}}{P_{\text{full}} - P_{\text{restricted}}}$$
(9)

where $SSE_{restricted} = sum$ of squared residuals of the restricted model; $SSE_{full} = sum$ of squared residuals of the full model; N = number of observations; $P_{full} = number$ of predictors in the full model; and $P_{restricted} = number$ of predictors in the restricted model. The F-statistic for comparing Model 4 and Model 1 was 22.11, the F-statistic for comparing Model 4 and Model 2 was 31.71, and the F-statistic for comparing Model 4 and Model 3 was 5.72. After looking up the F-distribution tables, we were 99% confident to reject the null hypotheses H_{01} and H_{02} , and 95% confident to reject the null hypothesis H_{03} . Thus, we concluded that Model 4 fit flow

Table 3. Generalized fundamental diagram estimation results

Variable description	Estimated parameter	t statistic
Constant, c	2,115.81	84.93
Traffic density, k (veh/km/ln)	-15.54	-33.19
Lane-changing rate, $lcr\left(100\% \times \frac{N^{LC}}{N^{veh}}\right)$	-274.53	-9.64
Lane-changing rate \times traffic density, $lr \times k$	12.49	8.91
Lane-changing rate \times traffic density ² , $lcr \times k^2$	-0.13	-8.05
Truck percentage, p_{truck}	-7.41	-2.07
Motorcycle percentage, p_{cycle}	8.37	2.41
No. of observations	58	36
Adjusted R^2		0.771

Source: Data from Federal Highway Administration (2005b).

rate statistically better than Models 1, 2, and 3. The detailed results of Model 4 (the generalized fundamental diagram) are presented in Table 3.

An adjusted R^2 of 0.771 indicated great estimation results. All independent variables and interaction terms were statistically significant, as suggested by the *t*-test values. Thus, the generalized fundamental diagram of the US101 data set was formulated as Eq. (10). Fig. 4 plots the generalized fundamental diagram when $p_{\rm truck} = 2.02$ and $p_{\rm cycle} = 0.76$ (i.e., observation mean values). The effect of each explanatory variable on flow rate is discussed below, respectively

$$q = 2,115.81 - 15.54 \times k - 274.53 \times lcr + 12.49 \times lcr \times k - 0.13 \times k^2 \times lcr - 7.41 \times p_{\text{truck}} + 8.37 \times p_{\text{cycle}}$$
 (10)

The marginal effect of traffic density on flow rate was formulated as Eq. (11) and is plotted in Fig. 5

$$\frac{\partial q}{\partial k} = -15.54 + 12.49 \times lcr - 0.26 \times k \times lcr \tag{11}$$

The marginal effect of traffic density on flow rate in the generalized fundamental diagram was no longer a constant as in the classic fundamental diagram but became a function of lane-changing rate and traffic density. When lane-changing rate equaled zero, the marginal effect of traffic density on flow rate equaled -15.54 veh/h/ln. Otherwise, when lane-changing rate was kept at a nonzero constant value, the marginal effect of traffic density on flow rate linearly decreased with a rate of $0.26 \times lcp$ as traffic density increased.

The marginal effect of lane changing on flow rate was formulated as Eq. (12) and is plotted in Fig. 6

$$\frac{\partial q}{\partial lcr} = -274.53 + 12.49 \times k - 0.13 \times k^2 \tag{12}$$

The marginal effect of lane changing on flow rate was a quadratic function of traffic density. This indicated that the effect varied as congestion developed (i.e., as traffic density increased), as

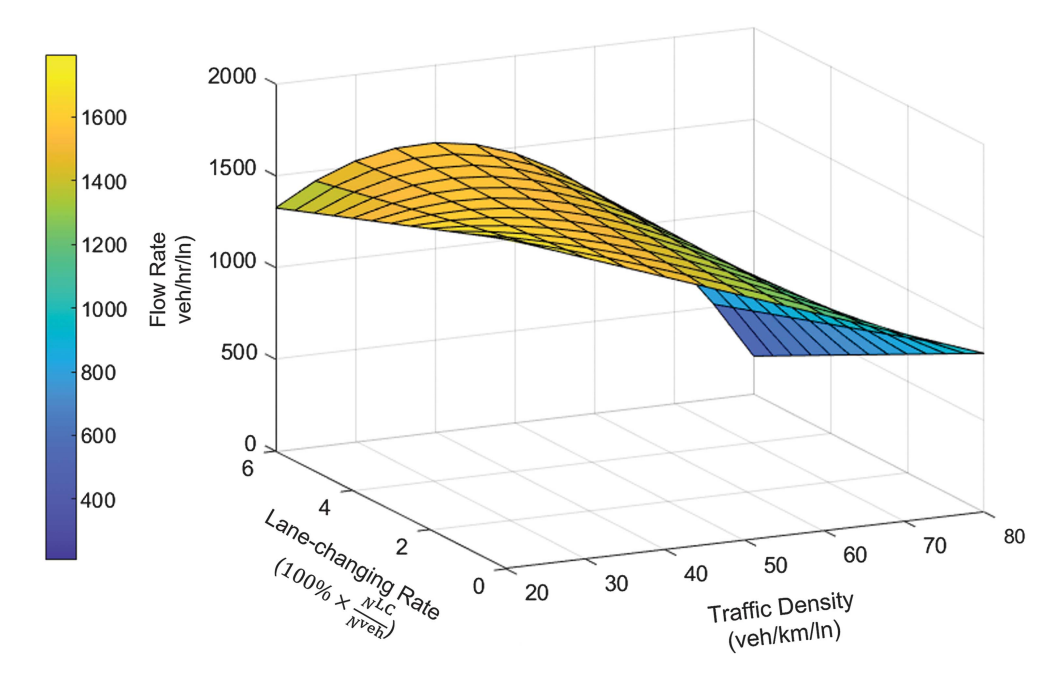


Fig. 4. Generalized fundamental diagram with fixed truck and motorcycle percentages. (Data from Federal Highway Administration 2005b.)

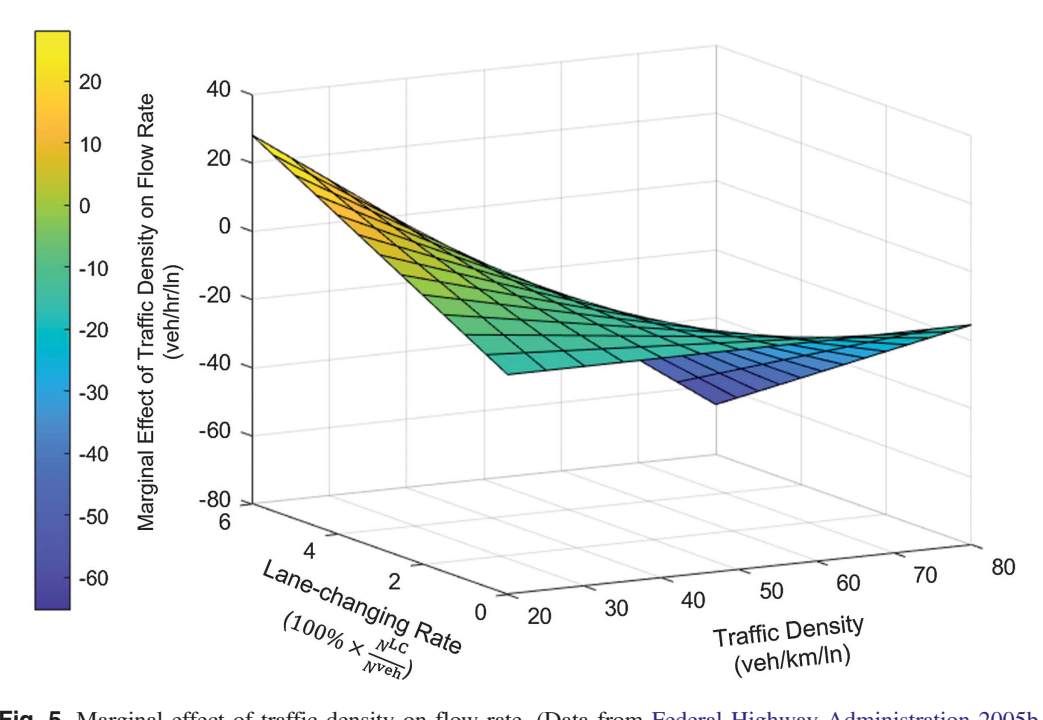


Fig. 5. Marginal effect of traffic density on flow rate. (Data from Federal Highway Administration 2005b.)

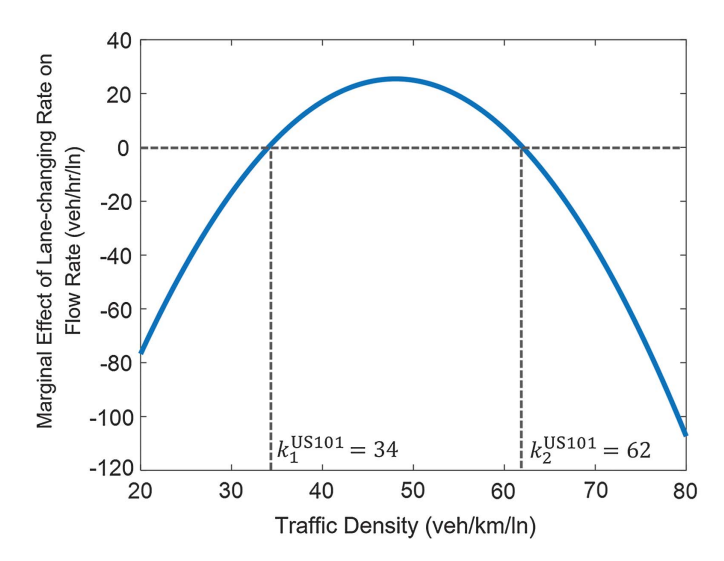
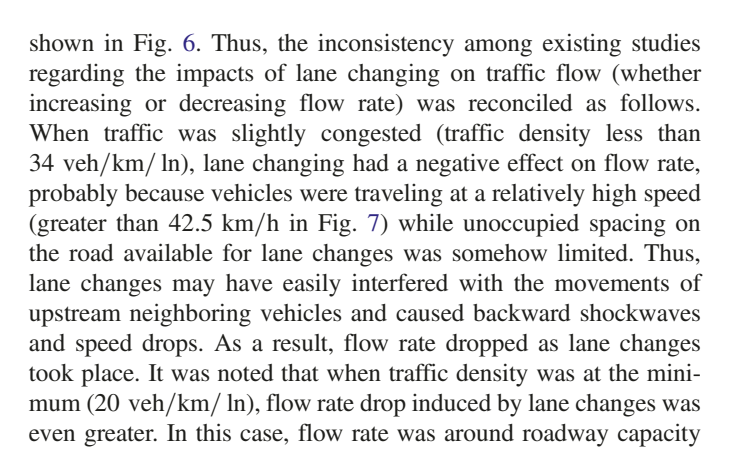


Fig. 6. Marginal effect of lane changing on flow rate. (Data from Federal Highway Administration 2005b.)



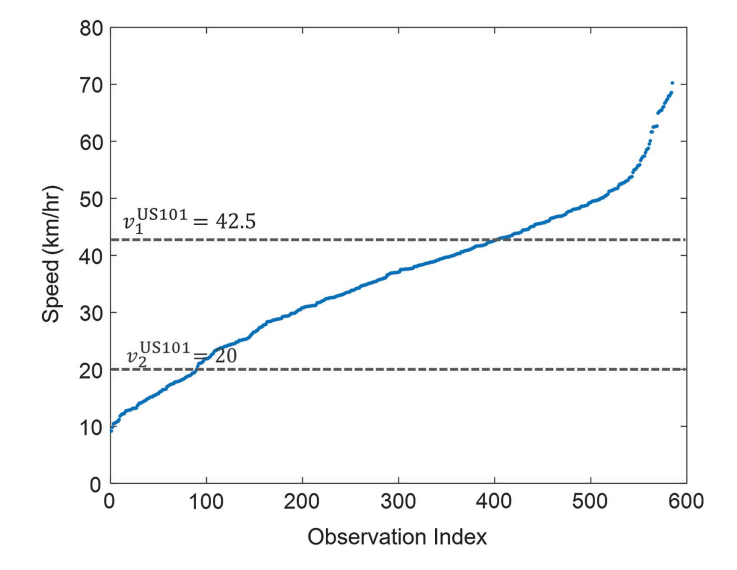


Fig. 7. Observation speed distribution. (Data from Federal Highway Administration 2005b.)

and overall traffic flow was stable. The disturbance caused by lane changes would easily break the stationary traffic state and result in a great flow rate drop. As the congestion evolved, the magnitude of flow rate drop decreased until traffic became moderately congested (traffic density between 34 veh/km/ln and 62 veh/km/ln). In this case, lane changing had a positive effect on flow rate. The corresponding average speed was not as high as in the previous case: between 20 km/h and 42.5 km/h in Fig. 7. In this speed range, a number of vehicles that desired to travel faster were already held in a platoon. They could thus take opportunities to change lanes to escape from the current oscillated traffic and improve their speed (Patire and Cassidy 2011). It was probable that the speed improvements of lane-changing vehicles offset the speed reductions of upstream neighboring vehicles and created a positive impact on overall traffic flow rate (Cheu et al. 2009; Li et al. 2006). None-theless, when traffic was heavily congested (traffic density greater than 62 veh/km/ln), lane changing again had a negative effect on flow rate. In this case, average speed was less than 20 km/h as shown in Fig. 7, and the unoccupied spacing for lane changes was very limited. Thus, lane changes may not have much improved the subject vehicles' speeds; rather, they caused more speed drops to upstream neighboring vehicles. As a result, collective flow rate decreased as lane changing increased. Intuitively, as traffic became more congested, flow rate dropped because lane changes became

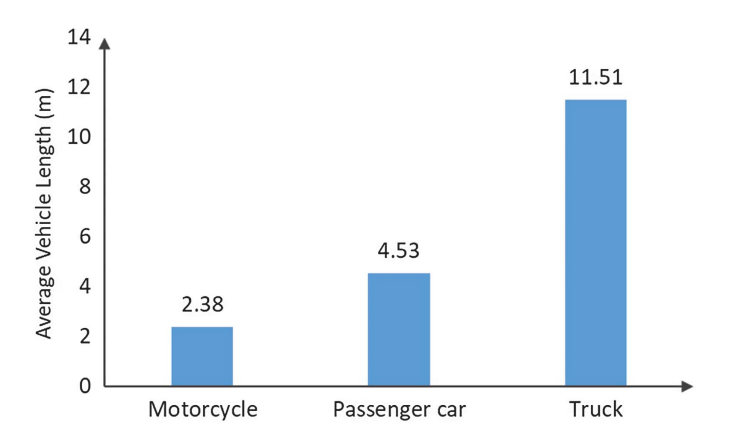


Fig. 8. Average vehicle length. (Data from Federal Highway Administration 2005b.)

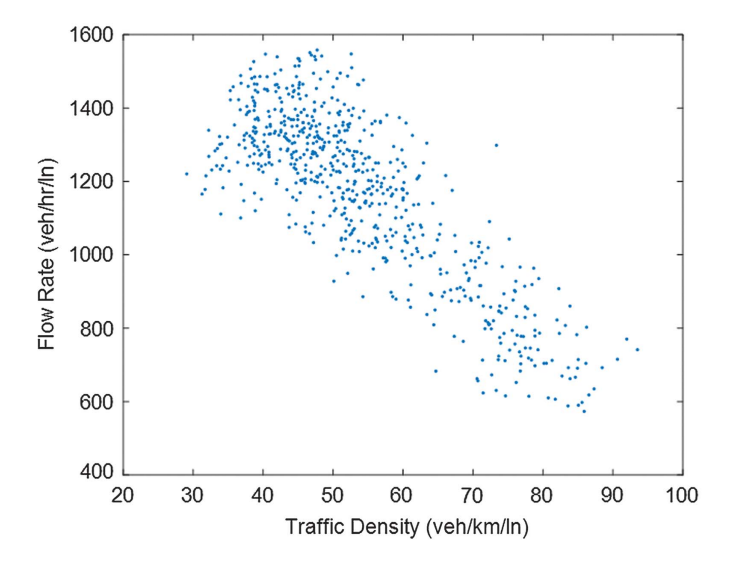


Fig. 9. Flow and density relationship. (Data from Federal Highway Administration 2005a.)

greater. This interesting finding shed light on creating new dynamic lane-changing management strategies to mitigate congestion. For example, we may allow for lane changes when traffic is moderately congested and restrict lane changes when traffic is slightly or severely congested.

The marginal effect of truck percentage on flow rate was -7.41 veh/h/ln. Thus, it was negatively correlated with traffic flow rate, indicating that a higher presence of trucks likely decreased traffic flow rate (Yang et al. 2015). A 1% increase in truck percentage would result in a decrease of 7.41 veh/h/ln in flow rate. Given the definition of flow rate—the number of vehicles passing through a given location on the roadway within a period (Treiber and Kesting 2013)—the longer the vehicle length, the smaller the flow rate. Fig. 8 shows the average vehicle lengths of three types of vehicles in the data set. Trucks were much longer than passenger cars, with an average length of 11.51 m (versus 4.53 m for cars), which supported the above explanation. Trucks' limited acceleration/deceleration capability also contributed to their negative impacts on traffic flow rate.

The marginal effect of motorcycle percentage on flow rate was 8.37 veh/h/ ln. Thus, motorcycle percentage was positively related to traffic flow rate compared with passenger cars. A 1% increase in motorcycle percentage would increase flow rate by 8.37 veh/h/ ln. This was an expected finding since motorcycles are physically shorter than cars, with an average length of 2.38 m and thus consume less roadway space. Besides, motorcycles have better acceleration/deceleration capabilities than passenger cars. Therefore, the presence of motorcycles contributes to higher flow rate (Meng et al. 2007; Minh and Sano 2003).

Model Spatial Transferability Assessment

This section assesses the spatial transferability of the generalized fundamental diagram. Models 1–4 were reevaluated using the NGSIM I-80 trajectory data set, which was collected in the San Francisco Bay Area in Emeryville, California, on April 13, 2005 (https://www.fhwa.dot.gov/publications/research/operations/06137/06137.pdf). The data aggregation strategy described earlier was also used to generate the I-80 observation set. The same parallelogram dimensions were used for consistency. The relationship of flow and density is plotted in Fig. 9. In total, 651 observations were obtained, 70% of which (456 regions) were used for model estimation and 30% (195 regions) for testing model prediction performance. The results are summarized in Table 4.

Similarly, accounting for heterogeneous traffic improved flow rate fitness and prediction accuracy, as shown in the results of Model 2. Considering lane-changing behavior also improved flow rate fitness and prediction accuracy, as shown in the results of Model 3. The best model performance was observed after incorporating both lane-changing behavior and heterogeneous traffic, as shown in the results of Model 4.

Table 4. Fundamental diagram model comparison

Model index	Model formulation	Adjusted R ²	RMSE (veh/h/ln)
1	$q = c + \alpha_1 \times k$	0.752	101.486
2	$q = c + \beta_1 \times k + \beta_2 \times p_{\text{truck}} + \beta_3 \times p_{\text{cycle}}$	0.790	91.725
3	$q = c + \gamma_1 \times k + \gamma_2 \times lcr + \gamma_3 \times lcr \times k + \gamma_4 \times k^2 \times lcr$	0.774	94.745
4	$q = c + \mu_1 \times k + \mu_2 \times lcr + \mu_3 \times lcr \times k + \mu_4 \times k^2 \times lcr + \mu_5 \times p_{\text{truck}} + \mu_6 \times p_{\text{cycle}}$	0.808	81.857

Source: Data from Federal Highway Administration (2005a).

Note: q = flow rate; k = traffic density; lcr = lane-changing rate; $p_{truck} =$ truck percentage; $p_{cycle} =$ motorcycle percentage; c = constant; α , β , γ , $\mu =$ model parameters; and $lcr \times k$, $lcr \times k^2 =$ interaction terms.

Table 5. Generalized fundamental diagram estimation results

	Estimated	
Variable description	parameter	t statistic
Constant, c	2,037.02	71.23
Traffic density, k (veh/km/ln)	-14.92	-32.94
Lane-changing rate, $lcr\left(100\% \times \frac{N^{LC}}{N^{veh}}\right)$	-338.72	-6.49
Lane-changing rate \times traffic density, $lc \times k$	12.61	6.44
Lane-changing rate \times traffic density ² , $lcr \times k^2$	-0.11	-6.06
Truck percentage, p_{truck}	-23.98	-9.33
Motorcycle percentage, p_{cycles}	8.67	1.99
Number of observations	45	56
Adjusted R^2		0.808

Source: Data from Federal Highway Administration (2005a).

Three hypothesis tests were conducted to test the superiority of Model 4 using the F-test. The three null hypotheses and three alternative hypotheses proposed in the previous section were used. The F-statistic for comparing Model 4 and Model 1 was 27.24, the F-statistic for comparing Model 4 and Model 2 was 14.87, and the F-statistic for comparing Model 4 and Model 3 was 43.57. After looking up the F-distribution tables, we were 99% confident to reject the null hypotheses H_{01} , H_{02} , and H_{03} . Thus, we concluded that Model 4 fit flow rate statistically better than Models 1, 2, and 3. The detailed estimation results of Model 4 (the generalized fundamental diagram) are presented in Table 5.

An adjusted R^2 of 0.808 indicated great estimation results. All independent variables and interaction terms were statistically significant. Thus, the generalized fundamental diagram of the I-80 data set was formulated as Eq. (13). Fig. 10 plots the generalized fundamental diagram when $p_{\rm truck}=4.38$ and $p_{\rm cycle}=1.05$ (i.e., observation mean values)

$$q = 2,037.02 - 14.92 \times k - 338.72 \times lcr + 12.61 \times lcp \times k$$
$$-0.11 \times k^2 \times lcr - 23.98 \times p_{\text{truck}} + 8.67 \times p_{\text{cycle}}$$
(13)

The marginal effect of traffic density on flow rate was formulated as Eq. (14) and is plotted in Fig. 11

$$\frac{\partial q}{\partial k} = -14.92 + 12.61 \times lcr - 0.22 \times k \times lcr \tag{14} \label{eq:14}$$

The parameters in the marginal effect of traffic density on flow rate in the I-80 model [Eq. (14)] were similar to those in the US101 model [Eq. (11)]. This indicated that the impact of traffic density on flow rate was consistent across different freeway segments.

The marginal effect of lane changing on flow rate was formulated as Eq. (15) and is plotted in Fig. 12

$$\frac{\partial q}{\partial lcr} = -338.72 + 12.61 \times k - 0.11 \times k^2 \tag{15}$$

While other parameters in the marginal effect of lane-changing on flow rate in the I-80 model [Eq. (15)] were similar to those in the US101 model [Eq. (12)], the constant terms in the two marginal effect functions were quite different (-338.72 versus -274.53). This was because US101 and I-80 had different congestion densities due to factors such as roadway characteristics (Bonneson et al. 2006) and driving behaviors (Toledo et al. 2007).

Based on the generated observations, US101's congestion density ranged from 20 to 80 veh/km/ln; I-80's congestion density ranged from 30 to 90 veh/km/ln. Despite the difference in these absolute values, the percentiles of the critical density values that separate positive and negative impacts of lane-changing on flow rate were similar between the two models. Thus, $k_1^{\rm US101}$ was at the 23rd percentile, $k_2^{\rm US101}$ was at the 70th percentile, $k_1^{\rm I80}$ was at the 22nd percentile, and $k_2^{\rm I80}$ was at the 70th percentile. This implied that the impact of lane changing on flow rate was consistent. When traffic density was relatively low or high, lane changing tended to decrease flow rate. However, when traffic density was in the middle range, lane changing tended to increase flow rate. These similar density percentiles can be used as future references to set density thresholds while developing dynamic lane-changing management strategies to mitigate congestion.

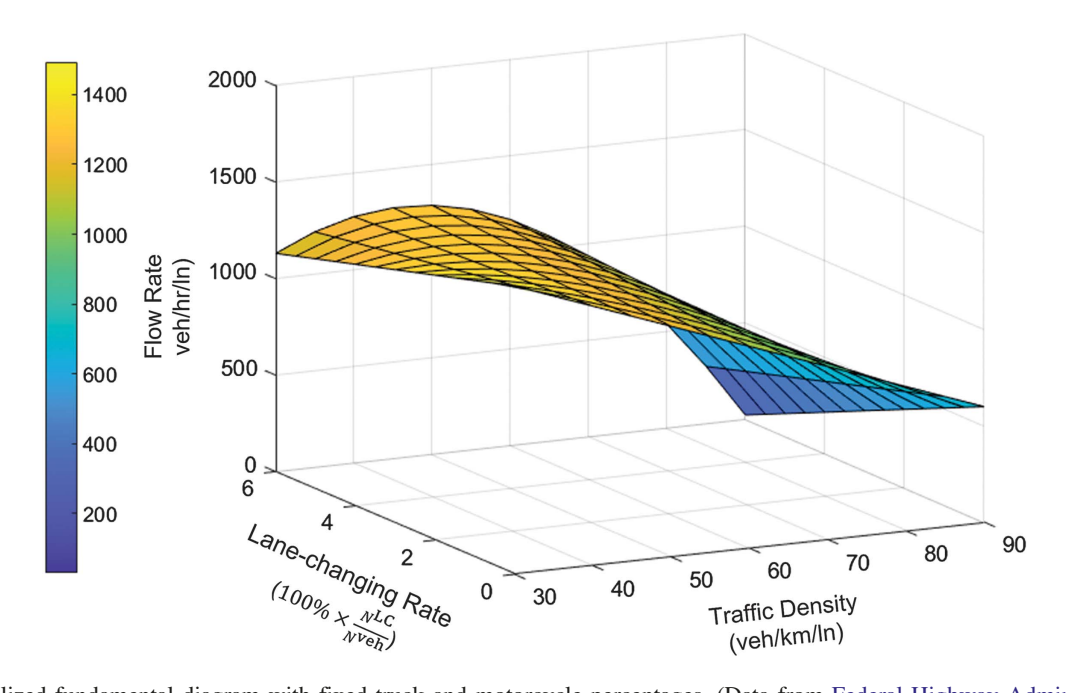


Fig. 10. Generalized fundamental diagram with fixed truck and motorcycle percentages. (Data from Federal Highway Administration 2005a.)

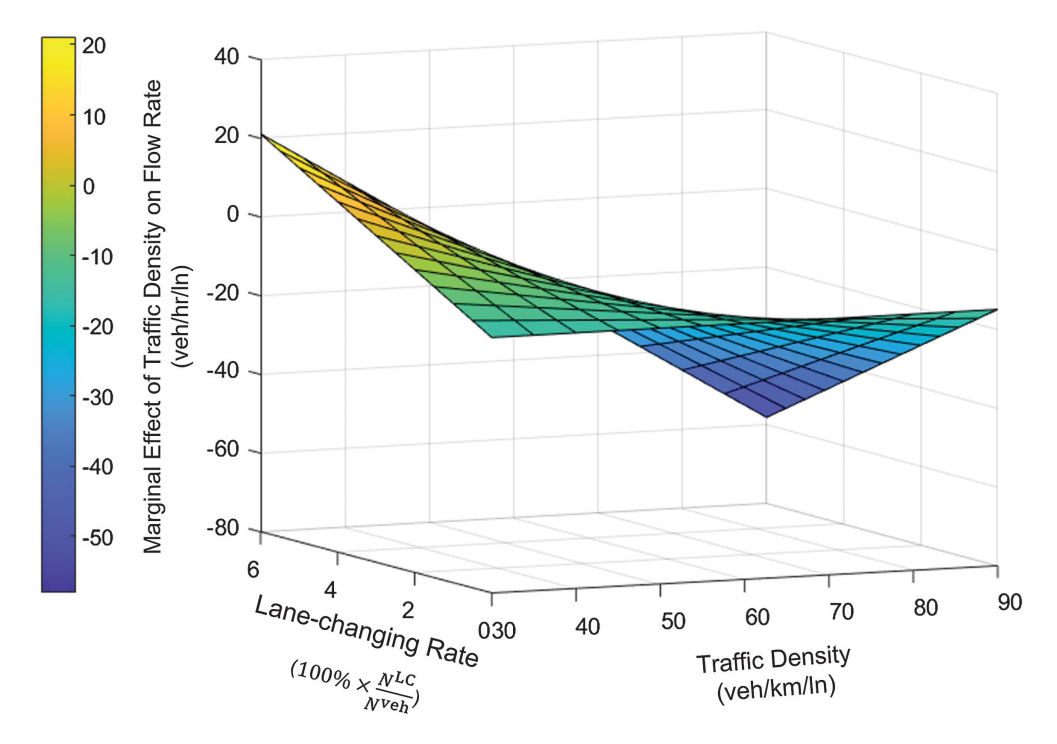


Fig. 11. Marginal effect of traffic density on flow rate. (Data from Federal Highway Administration 2005a.)

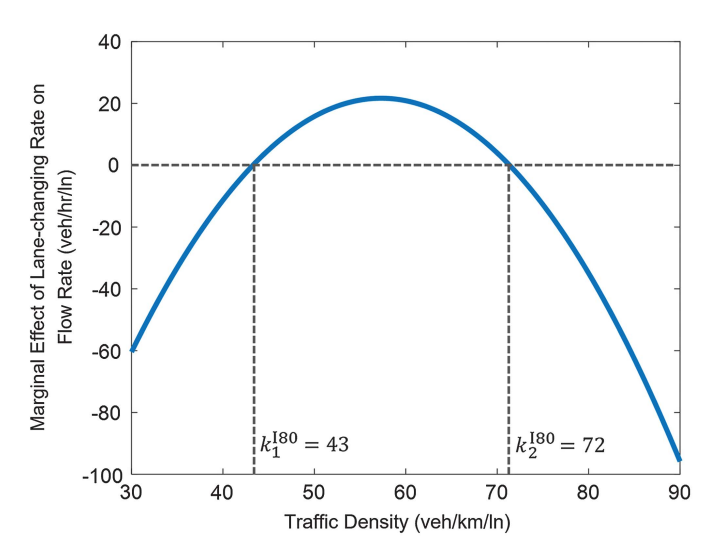


Fig. 12. Marginal effect of lane changing on flow rate. (Data from Federal Highway Administration 2005a.)

The marginal effect of truck percentage on flow rate in the I-80 model (-23.98 veh/h/ln in Table 5) was quite different from that in the US101 model (-7.41 veh/h/ln in Table 3). The presence of trucks on I-80 decreased flow rate much more than that on US101. Possible reasons follow. Traffic on I-80 was more congested than that on US101. Thus, the presence of trucks on I-80 likely degraded traffic performance more given trucks' inferior kinematic capability. Further, average truck length on I-80 was 14.78 m, as shown in Fig. 13, which was more than 3 m longer than that on US101. The longer the truck, the more roadway space it occupied and the worse its acceleration/deceleration capability. Therefore, longer trucks decreased flow rate more. This finding implied that not only vehicle type but also vehicle length should be carefully treated

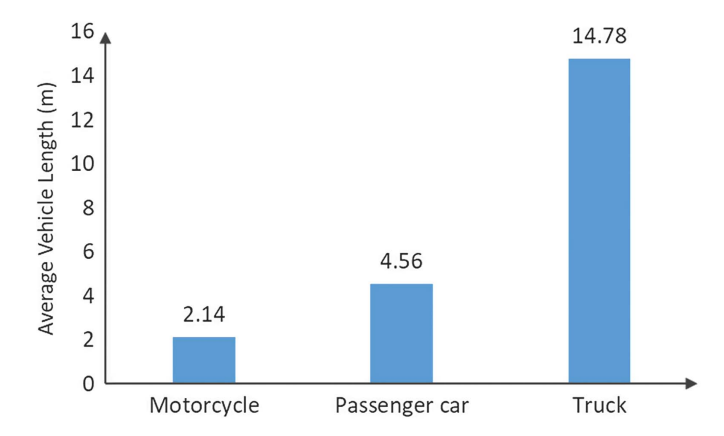


Fig. 13. Average vehicle length. (Data from Federal Highway Administration 2005a.)

while modeling heterogeneous traffic flow dynamics, especially for a vehicle type such as trucks with relatively dispersed vehicle lengths. In this study, the number of trucks within a parallelogram was not enough to further investigate the impact of truck length on the fundamental diagram. This might be an interesting research topic when more data sets containing various trucks are available.

Lastly, we saw that the marginal effect of motorcycle percentage on flow rate in the I-80 model (8.67 veh/h/ ln in Table 5) was similar to that in the US101 model (8.37 veh/h/ ln in Table 3). This was probably because the average motorcycle lengths were similar between US101 and I-80 (i.e., 2.14 versus 2.38 m).

Overall, the generalized fundamental diagram performed consistently between the US101 and I-80 data sets. A likelihood ratio test was conducted to assess the spatial transferability of the generalized fundamental diagram by calculating the \mathcal{X}^2 statistic (Washington et al. 2020)

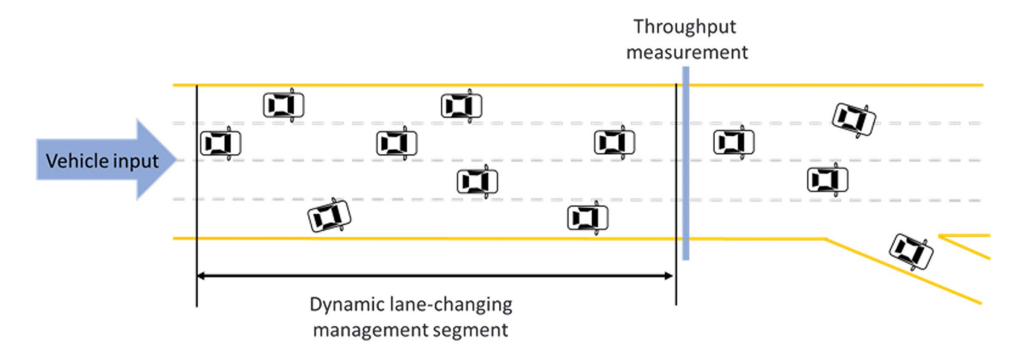


Fig. 14. Simulation segment.

$$\mathcal{X}^2 = -2 \times \left[LL(\boldsymbol{\beta_{both}}) - LL(\boldsymbol{\beta_{US101}}) - LL(\boldsymbol{\beta_{I80}}) \right] \tag{16}$$

where $LL(\beta_{both}) = log$ -likelihood at convergence of the model estimated with both US101 and I-80 data sets; $LL(\beta_{US101}) = log$ -likelihood at convergence of the model estimated with the US101 data set alone; and $LL(\beta_{180}) = log$ -likelihood at convergence of the model estimated with the I-80 data set alone. The \mathcal{X}^2 statistic was calculated as 59.84. The degree of freedom was computed as the number of predictors in the US101 model plus that in the I-80 model minus that in the combined data model, which was equal to 7. After looking up at \mathcal{X}^2 distribution table, we were 99% confident to claim that the generalized fundamental diagram was spatially transferable.

Dynamic Lane-Changing Management Strategy

The analysis described in this paper indicates that lane changes can decrease flow rate when traffic is slightly or severely congested but increase flow rate when traffic is moderately congested. The critical density values (k_1 and k_2) that separate positive and negative impacts of lane changing on congested flow rate are used to devise a dynamic lane-changing management strategy. When traffic is in a free-flow state, meaning that density is less than k_0 , lane changes are allowed. In this case, there is plenty of space in the roadway for downstream vehicles to absorb possible disturbances induced by lane changes. Thus, lane changes are not expected to affect traffic performance much. When traffic is congested and density is between k_1 and k_2 , lane changes are allowed, but when density is between k_0 and k_1 or greater than k_2 , lane changes are restricted. "Restricted" means "forbidden" unless they are mandatory such that vehicles can merge into the mainstream or exit the roadway. Variables k_0 , k_1 , and k_2 are determined by calibrating the generalized fundamental diagram with observed data when lane changes

To test the performance of the proposed strategy, a general freeway segment with four main lanes and one off-ramp was constructed in PTV VISSIM, as shown in Fig. 14. The off-ramp was added to generate congestion upstream, where the strategy was tested. The overall segment was about 3 km, and the testing segment was about 2 km. The simulation time was set as 30 min, and the vehicle input volume was time-dependent, increasing from 4,500 to 5,500 veh/h with a step size of 5 min. Referring to the vehicle composition of US101, 0.8% was set as motorcycles, 2% was set as trucks, and the remaining was set as passenger cars. The desired speed was 100 km/h. The diverging rate was 10%. It was assumed that diverging vehicles could make mandatory lane changes in the downstream segment to exit the freeway. Thus, lane changes in the testing segment were discretionary and could be

forbidden when necessary. The testing segment was configured not to reproduce the traffic of US101 but to test the effectiveness of the proposed strategy on a general freeway segment. The assumption was that the critical density percentiles of the proposed strategy would be generalizable at least with similar vehicle composition regardless of the specific fundamental diagram shape. This assumption was validated by the simulation results.

Three simulation cases were tested. In Case A, lane changes were forbidden at all times; in Case B, lane changes were allowed at all times; in Case C, lane changes were allowed when traffic was moderately ($k_1 \le \text{density} \le k_2$) congested and forbidden when traffic was slightly (density $< k_1$) or severely congested (density $> k_2$); k_1 and k_2 were set after calibrating the generalized fundamental diagram of the testing segment. As expected, they were at the 22nd and 71st percentiles, respectively, given that the vehicle composition of the testing segment was similar to that of US101. Lane changes were always allowed in the downstream segment. Traffic throughput was measured at the end of the testing segment, as shown in Fig. 14. Average speed and average delay were measured across the management segment. Each case was simulated 10 times, and performance measurements were averaged out. The simulation results are presented in Table 6.

The dynamic lane-changing management strategy produced the best mobility performance; second best was allowing all lane changes, and worst was restricting all lane changes. Specifically, compared with allowing all changes, the dynamic strategy improved traffic throughput, average speed, and average delay by 10.3%, 9.7%, and 19.2%, respectively. This finding suggests the promising benefits of this strategy in mitigating traffic congestion. The benefits are expected to increase as the study segment expands. It is noteworthy that the percentiles of density values that separate positive and negative impacts of lane changing may vary with some factors. Specifically, if the traffic stream is composed of a large number of trucks or motorcycles, the percentiles will be different from those in this study. The differences will be more significant when it comes to automated vehicles. Therefore, segment-specific generalized fundamental diagram calibration is very helpful for developing effective dynamic lane-changing management strategies and policies.

 Table 6. Strategy performance

Case	Throughput (veh/30 min)	Average speed (km/h)	Average delay (s)
A (no lane changes)	1,642	54.26	37.74
B (all lane changes)	2,047	73.35	23.17
C (dynamic strategy)	2,258	80.47	18.71

Conclusion

The classic triangular fundamental diagram is a fundamental theory to help understand traffic dynamics and so develop ways to mitigate congestion. However, it only focuses on vehicle longitudinal movements and may not fully capture vehicle lanechanging behavior. In addition, because it handles homogeneous traffic it cannot be directly applied to heterogeneous traffic. To address these limitations, this study generalized the diagram to consider lane-changing behavior and heterogeneous traffic using a generalized linear regression model. The NGSIM US101 trajectory data set was used for model estimation after aggregation. F-test results demonstrated that the generalized model fit and predicted flow rate better than the classic model. The impacts of lane-changing behavior on traffic flow varied as congestion developed. Lane changes decreased flow rate when traffic was slightly or severely congested but increased flow rate when traffic was moderately congested. This variation was captured by introducing terms for interaction between lane-changing rate and traffic density into the regression model.

The spatial transferability of the generalized model was verified with the NGSIM I-80 trajectory data set through a likelihood ratio test. It was shown that, although the congestion densities on US101 and I-80 were different, the percentiles of the critical density values that separated positive and negative impacts of lane changing on flow rate were similar between the US101 and I-80 models. These similar density percentiles could be used as future references to develop dynamic lane-changing management strategies to mitigate congestion, such as by setting density thresholds. It was also shown that the presence of trucks on I-80 decreased flow rate more significantly than that on US101. This probably can be attributed to trucks' longer average length and worse acceleration/ deceleration capability relative to cars. It implies that not only different vehicle types but also different vehicle lengths should be carefully considered when modeling heterogeneous traffic flow dynamics.

Motivated by the different impacts of lane changing on flow rate, a dynamic lane-changing management strategy was proposed to mitigate traffic congestion by restricting lane changes when traffic is slightly or severely congested. Simulation tests showed that the proposed strategy improves traffic throughput by 10.3%, average speed by 9.7%, and average delay by 19.2%, compared with the strategy of no restriction on lane changes. This exciting finding reveals the promising benefits of the dynamic lane-changing management strategy and provides implications for congestion mitigation.

This work can be extended in the following directions. The model results may be improved if we include more descriptive data in model estimation, such as driver, roadway, and weather characteristics. It might be interesting to investigate the impact of truck length on the fundamental diagram using data sets containing various trucks. Besides spatial transferability, the model's temporal transferability can be tested by comparing model estimation results using data from the same location but in a different period.

Data Availability Statement

The data is publicly available via https://ops.fhwa.dot.gov/trafficanalysistools/ngsim.htm. Some or all models or codes that support the findings of this study are available from the corresponding author upon reasonable request.

Acknowledgments

The authors thank Dr. Zhenyu Wang and Miss Runan Yang for providing insightful modeling suggestions. This research is sponsored by National Science Foundation through Grants CMMI #1558887 and CMMI #1932452.

References

- Aghabayk, K., S. Moridpour, W. Young, M. Sarvi, and Y.-B. Wang. 2011. "Comparing heavy vehicle and passenger car lane-changing maneuvers on arterial roads and freeways." *Transp. Res. Rec.* 2260 (1): 94–101. https://doi.org/10.3141/2260-11.
- Ali, Y., M. M. Haque, Z. Zheng, S. Washington, and M. Yildirimoglu. 2019. "A hazard-based duration model to quantify the impact of connected driving environment on safety during mandatory lane-changing." Transp. Res. Part C Emerging Technol. 106: 113–131. https://doi.org/10.1016/j.trc.2019.07.015.
- Bonneson, J. A., B. Nevers, M. P. Pratt, and G. Bonyani. 2006. "Influence of area population, number of lanes, and speed limit on saturation flow rate." *Transp. Res. Rec.* 1988 (1): 76–85. https://doi.org/10.1177/0361198106198800110.
- Bun, M. J. G., and T. D. Harrison. 2019. "OLS and IV estimation of regression models including endogenous interaction terms." *Econ. Rev.* 38 (7): 814–827. https://doi.org/10.1080/07474938.2018.1427486.
- Cheu, R. L., J. Martinez, and C. Duran. 2009. "A cell transmission model with lane changing and vehicle tracking for port of entry simulations." *Transp. Res. Rec.* 2124 (1): 241–248. https://doi.org/10.3141/2124-24.
- Coifman, B., S. Krishnamurthy, and X. Wang. 2005. "Lane-change maneuvers consuming freeway capacity." In *Proc., Traffic and Granular Flow* '03, 3–14. New York: Springer.
- Cortina, J. M. 1993. "Interaction, nonlinearity, and multicollinearity: Implications for multiple regression." *J. Manage.* 19 (4): 915–922. https://doi.org/10.1177/014920639301900411.
- Eliasson, J. 2021. "Efficient transport pricing—Why, what, and when?" *Commun. Transp. Res.* 1 (Dec): 100006. https://doi.org/10.1016/j.commtr.2021.100006.
- Federal Highway Administration. 2005a. "Interstate 80 freeway dataset." Accessed April 1, 2020. https://www.fhwa.dot.gov/publications/research/operations/06137/.
- Federal Highway Administration. 2005b. "US highway 101 dataset." Accessed April 1, 2020. https://www.fhwa.dot.gov/publications/research/operations/07030/index.cfm.
- Gu, X., M. Abdel-Aty, Q. Xiang, Q. Cai, and J. Yuan. 2019. "Utilizing UAV video data for in-depth analysis of drivers' crash risk at interchange merging areas." Accid. Anal. Prev. 123 (Nov): 159–169. https://doi.org/10.1016/j.aap.2018.11.010.
- Gupta, A. K., and V. K. Katiyar. 2007. "A new multi-class continuum model for traffic flow." *Transportmetrica* 3 (1): 73–85. https://doi.org/10.1080/18128600708685665.
- Jin, W.-L. 2010a. "A kinematic wave theory of lane-changing traffic flow." Transp. Res. Part B Methodol. 44 (8–9): 1001–1021. https://doi.org/10.1016/j.trb.2009.12.014.
- Jin, W.-L. 2010b. "Macroscopic characteristics of lane-changing traffic." Transp. Res. Rec. 2188 (1): 55–63. https://doi.org/10.3141/2188-07.
- Jin, W.-L. 2013. "A multi-commodity Lighthill-Whitham-Richards model of lane-changing traffic flow." *Procedia-Soc. Behav. Sci.* 80 (Jun): 658– 677. https://doi.org/10.1016/j.sbspro.2013.05.035.
- Karaca-Mandic, P., E. C. Norton, and B. Dowd. 2012. "Interaction terms in nonlinear models." *Health Serv. Res.* 47 (1pt1): 255–274. https://doi.org/10.1111/j.1475-6773.2011.01314.x.
- Khan, S. I., and P. Maini. 1999. "Modeling heterogeneous traffic flow." *Transp. Res. Rec.* 1678 (1): 234–241. https://doi.org/10.3141/1678-28.
- Knoop, V. L., S. P. Hoogendoorn, Y. Shiomi, and C. Buisson. 2012. "Quantifying the number of lane changes in traffic: Empirical analysis." Transp. Res. Rec. 2278 (1): 31–41. https://doi.org/10.3141/2278-04.
- Laval, J. A. 2011. "Hysteresis in traffic flow revisited: An improved measurement method." *Transp. Res. Part B Methodol.* 45 (2): 385–391. https://doi.org/10.1016/j.trb.2010.07.006.

- Laval, J. A., and B. R. Chilukuri. 2016. "Symmetries in the kinematic wave model and a parameter-free representation of traffic flow." *Transp. Res. Part B Methodol*. 89 (Jul): 168–177. https://doi.org/10.1016/j.trb.2016 02.009
- Laval, J. A., and C. F. Daganzo. 2006. "Lane-changing in traffic streams." Transp. Res. Part B Methodol. 40 (3): 251–264. https://doi.org/10.1016/j.trb.2005.04.003.
- Li, Q., X. Li, and F. Mannering. 2021. "Assessment of discretionary lane-changing decisions using a random parameters approach with heterogeneity in means and variances." *Transp. Res. Rec.* 2675 (6): 330–338. https://doi.org/10.1177/0361198121992364.
- Li, X.-G., B. Jia, Z.-Y. Gao, and R. Jiang. 2006. "A realistic two-lane cellular automata traffic model considering aggressive lane-changing behavior of fast vehicle." *Physica A* 367 (Jul): 479–486. https://doi. org/10.1016/j.physa.2005.11.016.
- Logghe, S., and L. H. Immers. 2008. "Multi-class kinematic wave theory of traffic flow." Transp. Res. Part B Methodol. 42 (6): 523–541. https://doi. org/10.1016/j.trb.2007.11.001.
- Ludden, T. M., S. L. Beal, and L. B. Sheiner. 1994. "Comparison of the Akaike Information Criterion, the Schwarz criterion and the F test as guides to model selection." *J. Pharmacokinet. Biopharm.* 22 (5): 431–445. https://doi.org/10.1007/BF02353864.
- Mason, A. D., and A. W. Woods. 1997. "Car-following model of multispecies systems of road traffic." *Phys. Rev. E* 55 (3): 2203. https://doi.org/10.1103/PhysRevE.55.2203.
- Meng, J., S. Dai, L. Dong, and J. Zhang. 2007. "Cellular automaton model for mixed traffic flow with motorcycles." *Physica A* 380 (Jul): 470–480. https://doi.org/10.1016/j.physa.2007.02.091.
- Minh, C. C., and K. Sano. 2003. "Analysis of motorcycle effects to saturation flow rate at signalized intersection in developing countries." J. Eastern Asia Soc. Transp. Stud. 5 (Oct): 1211–1222.
- Newell, G. F. 1993. "A simplified theory of kinematic waves in highway traffic, part I: General theory." *Transp. Res. Part B Methodol.* 27 (4): 281–287. https://doi.org/10.1016/0191-2615(93)90038-C.
- Patire, A. D., and M. J. Cassidy. 2011. "Lane changing patterns of bane and benefit: Observations of an uphill expressway." *Transp. Res. Part B Methodol*. 45 (4): 656–666. https://doi.org/10.1016/j.trb.2011.01.003.
- Peeta, S., P. Zhang, and W. Zhou. 2005. "Behavior-based analysis of free-way car-truck interactions and related mitigation strategies." *Transp. Res. Part B Methodol.* 39 (5): 417–451. https://doi.org/10.1016/j.trb.2004.06.002.
- Pompigna, A., and F. Rupi. 2015. "Differences between HCM procedures and fundamental diagram calibration for operational LOS assessment on Italian freeways." *Transp. Res. Procedia* 5: 103–118. https://doi .org/10.1016/j.trpro.2015.01.016.
- Qian, Z. S., J. Li, X. Li, M. Zhang, and H. Wang. 2017. "Modeling heterogeneous traffic flow: A pragmatic approach." *Transp. Res. Part B Methodol*. 99 (May): 183–204. https://doi.org/10.1016/j.trb.2017.01 .011.

- Qu, X., J. Zhang, and S. Wang. 2017. "On the stochastic fundamental diagram for freeway traffic: Model development, analytical properties, validation, and extensive applications." *Transp. Res. Part B Methodol*. 104 (Oct): 256–271. https://doi.org/10.1016/j.trb.2017.07.003.
- Shvetsov, V., and D. Helbing. 1999. "Macroscopic dynamics of multilane traffic." *Phys. Rev. E* 59 (6): 6328. https://doi.org/10.1103/PhysRevE .59.6328.
- Toledo, T., H. N. Koutsopoulos, and M. Ben-Akiva. 2007. "Integrated driving behavior modeling." *Transp. Res. Part C Emerging Technol.* 15 (2): 96–112. https://doi.org/10.1016/j.trc.2007.02.002.
- Treiber, M., and A. Kesting. 2013. "Traffic flow dynamics." In *Traffic flow dynamics: Data, models and simulation*. Berlin: Springer.
- van Winsum, W., D. De Waard, and K. A. Brookhuis. 1999. "Lane change manoeuvres and safety margins." *Transp. Res. Part F Traffic Psychol. Behav.* 2 (3): 139–149. https://doi.org/10.1016/S1369-8478 (99)00011-X.
- Washington, S., M. G. Karlaftis, F. Mannering, and P. Anastasopoulos. 2020. Statistical and econometric methods for transportation data analysis. Boca Raton, FL: CRC Press.
- Yang, D., X. Qiu, D. Yu, R. Sun, and Y. Pu. 2015. "A cellular automata model for car–truck heterogeneous traffic flow considering the car– truck following combination effect." *Physica A* 424 (Apr): 62–72. https://doi.org/10.1016/j.physa.2014.12.020.
- Zhang, C., N. R. Sabar, E. Chung, A. Bhaskar, and X. Guo. 2019. "Optimisation of lane-changing advisory at the motorway lane drop bottleneck." *Transp. Res. Part C Emerging Technol.* 106 (Sep): 303–316. https://doi.org/10.1016/j.trc.2019.07.016.
- Zhang, H. M., and W. L. Jin. 2002. "Kinematic wave traffic flow model for mixed traffic." Transp. Res. Rec. 1802 (1): 197–204. https://doi.org/10 .3141/1802-22.
- Zhang, J., X. Qu, and S. Wang. 2018. "Reproducible generation of experimental data sample for calibrating traffic flow fundamental diagram." Transp. Res. Part A Policy Pract. 111 (May): 41–52. https://doi.org/10.1016/j.tra.2018.03.006.
- Zheng, Z. 2014. "Recent developments and research needs in modeling lane changing." *Transp. Res. Part B Methodol.* 60 (Feb): 16–32. https://doi.org/10.1016/j.trb.2013.11.009.
- Zheng, Z. 2021. "Reasons, challenges, and some tools for doing reproducible transportation research." *Commun. Transp. Res.* 1 (Dec): 100004. https://doi.org/10.1016/j.commtr.2021.100004.
- Zheng, Z., S. Ahn, D. Chen, and J. Laval. 2013. "The effects of lane-changing on the immediate follower: Anticipation, relaxation, and change in driver characteristics." *Transp. Res. Part C Emerging Technol.* 26 (Jan): 367–379. https://doi.org/10.1016/j.trc.2012.10.007.
- Zhou, J., L. Rilett, and E. Jones. 2019. "Estimating passenger car equivalent using the HCM-6 PCE methodology on four-lane level freeway segments in western US." *Transp. Res. Rec.* 2673 (11): 529–545. https://doi.org/10.1177/0361198119851448.